Rotating field entropy change in hexagonal $TmMnO_3$ single crystal with anisotropic paramagnetic response

Jin-Ling Jin, Xiang-Qun Zhang, Heng Ge, and Zhao-Hua Cheng*

State Key Laboratory of Magnetism, Institute of Physics, Chinese Academy of Sciences, Beijing 100190, People's Republic of China

(Received 16 February 2012; revised manuscript received 26 April 2012; published 21 June 2012)

The anisotropy of magnetic field-induced entropy change, $-\Delta S$, was investigated in a hexagonal $TmMnO_3$ single crystal at a temperature range of 2–50 K. The value of $-\Delta S$ along the c axis reaches a maximum of 8.73 J/kg K at 17 K in a field of 70 kOe, which is 20 times larger than that along the a axis. Our finding suggests that the rotating field entropy change $-\Delta S^{R}(\alpha)$ from the a to c axis is attributed not only to magnetocrystalline anisotropy, but to thermal fluctuations.

DOI: 10.1103/PhysRevB.85.214426 PACS number(s): 75.47.Lx, 75.30.Sg, 75.30.Gw

I. INTRODUCTION

The magnetocaloric effect (MCE) is currently attracting considerable interest from both fundamental and practical points of view. Magnetic refrigeration has potential application in many fields due to combined energy and environmental advantages. In the last decades, MCE research has mainly focused on materials with magnetic phase transitions involving the paraprocess[1–4] under magnetic field variation near the transition temperature. Alternatively, magnetic refrigeration can also be achieved by a rotating field MCE based on changing the magnetic anisotropy energy in a constant magnetic field,[5] which is attractive due to the simplification and possible miniaturization of the device.[6] Recently, this kind of MCE is explored in $NdCo_5$,[5] $BaCo_{0.62}Zn_{1.38}Fe_{16}O_{27}$,[7] and $Er_2Fe_{14}B$,[8] single-crystal near-spin reorientation transition in the vicinity of room temperature. However, it is also meaningful to study low-temperature refrigerants for ultralow-temperature refrigeration. Recently, giant rotating field entropy change, which is dominated by magnetocrystalline anisotropy, was observed in a single crystal of orthorhombic $TbMnO_3$ at low temperature.[9] On the basis of a single ion anisotropy model, magnetocrystalline anisotropy is determined not only by the $4f$ charge distribution of R^{3+} ions, but also by the crystal structure.[10,11] The investigation of rotating field entropy change, $-\Delta S^{R}$, in materials with various R^{3+} ions and structures can give a deeper insight into the contribution of magnetocrystalline anisotropy to the rotating field MCE effect.

In this paper, we investigated the rotating field entropy change in a $TmMnO_3$ single crystal. The reason for choosing a $TmMnO_3$ single crystal is twofold. First, the prolaticity of the Tm^{3+} ion $4f$ electron cloud is significantly different from that of the Tb^{3+} ion (i.e., the first one is oblate and the last one is prolate); consequently, a change of sign for single-ion anisotropy is expected.[12] Second, in contrast to $TbMnO_3$, $TmMnO_3$ has a hexagonal structure with $P6_3cm$ symmetry under normal pressure.[13] $TmMnO_3$ belongs to the series of hexagonal $RMnO_3$ (R = Ho-Lu) compounds, where Mn^{3+} ions form geometrically frustrated triangular sublattice packed along the c axis.[14] The magnetic frustration of the Mn^{3+} sublattice arises from the triangular geometry[15] and forms 120° antiferromagnetic (AFM) ordering at low temperature.[14] The Neel temperature in $TmMnO_3$ is reported to be 81 K[16] for ceramics and 82 K[17] and 84 K[18] for single crystals. However, this transition is not obvious in thermal magnetization curves because it is suppressed by the dominant Tm^{3+} moments. This noncollinear magnetic structure is very stable, even in a magnetic field of 10 T.[18] Unlike the Mn^{3+} sublattice, the magnetic ordering of Tm^{3+} ions in $TmMnO_3$ cannot be identified above 1.8 K from thermal magnetization curves.[18] However, Mössbauer spectra reveal that magnetic moments of Tm^{3+} at $4b$ sites partially order along the c direction below the ordering temperature of Mn^{3+} due to the Tm-Mn interaction, whereas the moments at $2a$ sites remain paramagnetic down to 4.2 K.[19] Notably, crystal field plays an important role in the low-temperature range,[19,20] which may generate significant magnetic anisotropy. Owing to the anisotropic paramagnetic response, we find that magnetocrystalline anisotropy alone is insufficient to fit the rotating field entropy change, and thermal fluctuations should be taken into account in hexagonal $TmMnO_3$ single crystals.

II. EXPERIMENTAL

$TmMnO_3$ ceramic was prepared with the starting material Tm_2O_3 (>99.9%) and MnO_2 (99.9%). Then, it was pressed into pellets and sintered in air for 48 hours using the solid-state reaction method at 1200 °C. X-ray diffraction (XRD) showed the prepared sample was single phase with $P6_3cm$ crystallographic symmetry. The ceramic was compressed into rods under hydrostatic pressure and sintered at 1400 °C for 48 hours. A $TmMnO_3$ single crystal was grown by the floating zone method with four ellipsoidal mirrors (Crystal Systems Inc., FZ-T-10000-H-VI-VP). A back-reflection Laue XRD experiment was carried out to check the single crystallinity and determine the crystallographic direction. Magnetization measurements were performed on a commercial superconducting quantum interference device (SQUID) magnetometer (Quantum Design, MPMS-XL).

III. RESULTS AND DISCUSSION

The thermal magnetization curves along the a and c axes of the $TmMnO_3$ single crystal are shown in Figs. 1(a) and 1(b), respectively. The measurements were carried out in a field of 100 Oe after zero-field cooling (ZFC) and field cooling (FC), respectively. As illustrated in the insets of Figs. 1(a) and 1(b), the inverse magnetization vs temperature curves above 200 K were fitted by a Curie–Weiss law. Significantly

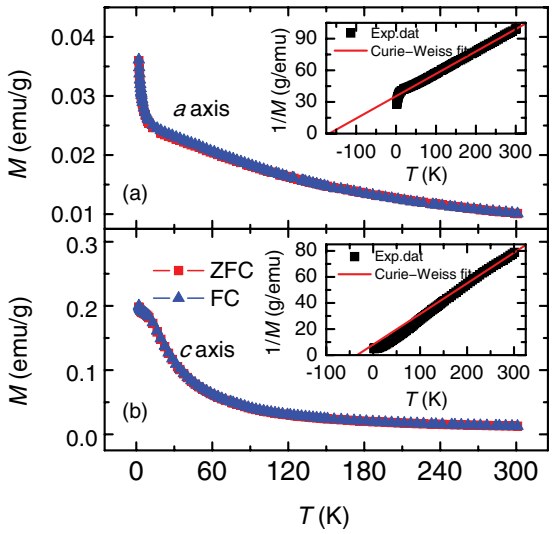

FIG. 1. (Color online) Thermal magnetization curves along the a axis (a) and c axis (b) in a field of 100 Oe. ZFC and FC curves are shown as red and blue dotted lines, respectively. The inset shows the $1/M$ and temperature relation with the corresponding Curie–Weiss fitting curves.

large anisotropy can be discerned from the fitted Curie–Weiss temperature, -168 and -35 K for a and c axes, respectively. An early report explained that the anisotropic Curie–Weiss temperature between the two directions was caused by the aspherical crystal field of Tm^{3+} ions.[21] The negative Curie–Weiss temperature reflects the AFM interaction in the system. Due to the paramagnetic behavior of Tm^{3+} ions, as discussed below, a steep increase in magnetization was observed with decreasing temperature, implying that a large change in entropy could be expected.

Figures 2(a) and 2(b) describe the representative isothermal magnetization curves along the a and c axes of the $TmMnO_3$ single crystal in a field up to 70 kOe with a step of 2 kOe and in a temperature range from 2 to 50 K with an interval of 2 K. Data for increasing and decreasing the magnetic field at 2 K, as shown in each figure, demonstrate a little hysteresis loss in

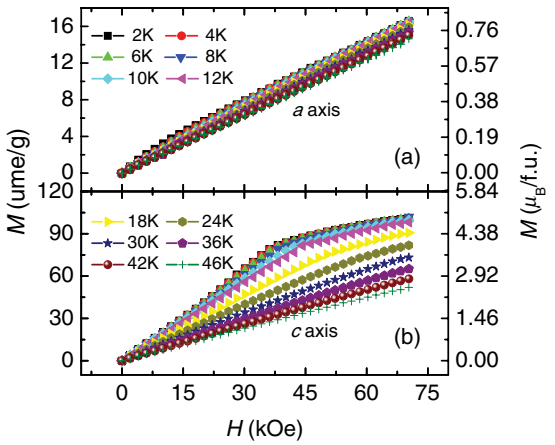

FIG. 2. (Color online) Representative magnetization isothermals for the (a) a axis and (b) c axis in a temperature range of 2–50 K. Both increasing and decreasing field results are shown at 2 K.

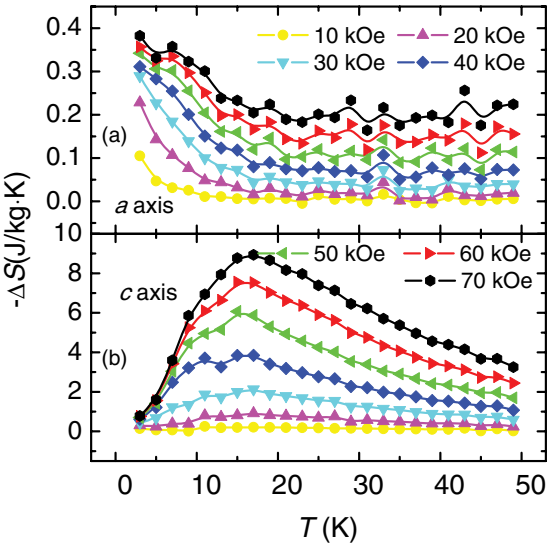

FIG. 3. (Color online) Magnetic entropy change ΔS as a function of temperature for the (a) a axis and (b) c axis in various magnetic fields.

the cycling process. A much larger value of magnetization was observed along the c axis with a magnitude of 4.9 μ_B per unit cell in 70 kOe at 2 K.

Magnetic field–induced entropy change $-\Delta S$ was calculated from the isothermal curves with the following equation based on a Maxwell relation

$$\Delta S(T,H) = \int_0^H \left(\frac{\partial M}{\partial T}\right)_H dH = \sum_0^H \left(\frac{M|_{T+\Delta T} - M|_{T-\Delta T}}{(T+\Delta T)-(T-\Delta T)}\right)_H \Delta H, \quad (1)$$

where the second term is used for numerical calculation by using the slope of two adjacent data points to approximate the gradient of $(\partial M/\partial T)_H$. In this case, $\Delta T = 1$ K and $\Delta H = 2$ kOe, from which the calculated $-\Delta S$ vs temperature is shown in Figs. 3(a) and 3(b) for a field along the a and c axes, respectively. Peaks appear within the range $15 \sim 17$ K for the c axis with a value of 8.73 J/kg K in a field of 70 kOe, whereas $-\Delta S$ for the a axis is almost zero in the whole temperature range.

We use the rule suggested by Gschneidner *et al.*[22] to calculate the refrigeration capacity (RC) by integrating the area under $-\Delta S$ vs T curves, using the temperature range at half-maximum of the peak (Fig. 4). The two directions manifest obvious anisotropy with values of RC in a field of 70 kOe equal to 6.2 J/kg and 211.6 J/kg for a and c axes, respectively. Single crystal with anisotropic MCE is a promising choice for the new type of magnetic refrigeration by simply rotating the magnetic field or refrigerants.

In order to investigate the rotating field entropy change ΔS^R at 16 K where the entropy change shows the largest anisotropy, we measured the isothermal magnetization at adjacent temperatures 15 and 17 K ($\Delta T = 1$ K) in fields up to 50 kOe with a step of 2 kOe ($\Delta H = 2$ kOe) applied along the ac plane separated by 10°, in the c to a direction. We define that $\alpha = 0°$ and 90° denote the c and a directions.

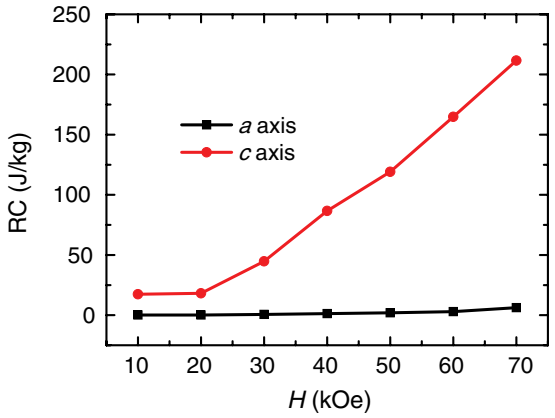

FIG. 4. (Color online) Refrigeration capacity (RC) for (a) the a axis and (b) c axis vs magnetic field.

These are displayed in Fig. 5. The entropy change $\Delta S(\alpha)$ for each angle α at 16 K in a field of 50 kOe can be calculated by Eq. (1) using the data in Fig. 5. By choosing a direction as the starting angle, the rotating field entropy change $\Delta S^{\mathrm{R}}(\alpha)$ at 16 K can be expressed as the equation

$$\Delta S^{\mathrm{R}}(\alpha) = \Delta S(\alpha) - \Delta S(90^{\circ}). \tag{2}$$

In Fig. 6(b), $-\Delta S^{\mathrm{R}}(\alpha)$ in a field of 50 kOe is shown as squares. A gradual increase in $-\Delta S^{\mathrm{R}}(\alpha)$ can be seen as the magnetic field is rotated from the a to c axis and reaches a maximum value of 5 J/kg K.

We try to build the direct bridge between the rotating field entropy change $-\Delta S^{\mathrm{R}}(\alpha)$ and the magnetocrystalline anisotropy in the $TmMnO_3$ single crystal. By using the coherent rotation model described in Ref. 9, the magnetocrystalline anisotropy constant at 16 K is obtained by fitting the magnetization curve for the hard axis (a axis), which is shown in the inset of Fig. 6(a). The corresponding result for the rotating field entropy change is displayed in Fig. 6(b) as a blue line. As shown in Fig. 6(b), the fitting values are much smaller than the experimental data, suggesting that the

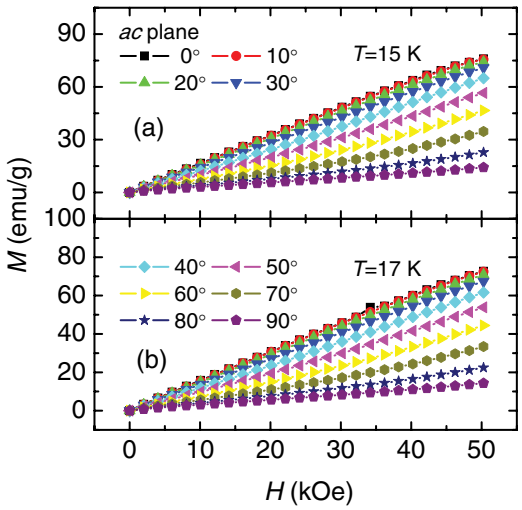

FIG. 5. (Color online) Isothermal magnetization curves within the ac plane at (a) 15 K and (b) 17 K. 90°and 0° correspond to the a and c directions, respectively.

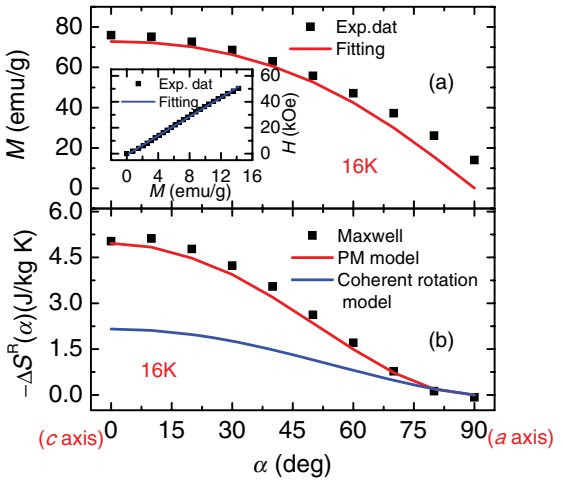

FIG. 6. (Color online) (a) Rotating magnetization curve from the a to c axis in a field of 50 kOe at 16 K with the experimental result (squares) and fitted curve (line). The inset shows the fitted hard axis (a axis) magnetization. (b) Rotating field entropy change $-\Delta S^{\mathrm{R}}(\alpha)$ from the a to c axis in a field of 50 kOe at 16 K. The result from isothermal magnetization curves is shown as squares. The blue and red lines represent the results from the coherent rotation and PM models, respectively.

magnetocrystalline anisotropy constant is underestimated, and an additional contribution to rotating field entropy change should be considered.

Due to the stable magnetic structure of Mn^{3+} in a high magnetic field, Tm^{3+} makes a major contribution to the magnetization in $TmMnO_3$. However, the magnetic ordering of R^{3+} in the hexagonal $RMnO_3$ family generally arises at a much lower temperature than Mn^{3+} due to the weaker R-R exchange interaction.[23,24] As reported in Ref. 19, only the Tm^{3+} magnetic moments at 4b sites order partially, whereas those at 2a sites are totally paramagnetic down to 4.2 K. $TmMnO_3$ shows linearly increasing magnetization with magnetic field at 16 K, which is also a sign of paramagnetic behavior in Tm^{3+} moments. Because of the highly paramagnetic (PM) behavior, the coherent rotation model is not enough to describe the entropy change in our system. Here, we introduce the PM model in which we use a Boltzmann distribution to assign spin direction.

The a and c directions are taken as the x and z axes in the spherical coordinate system. Because the rotating magnetization curve shown in Fig. 6(a) is sinusoidal, we keep the first two terms in magnetocrystalline anisotropy energy. First, we can write the unitary condition as

$$A_0 \iint \exp\left(-\frac{K_1 \sin^2\theta + K_2 \sin^4\theta - \mu_B g J \times H \cos\Gamma}{k_B T}\right) \times d\theta d\phi = 1, \tag{3}$$

where A_0 is the unitary constant, K_1 and K_2 are the first- and second-order magnetocrystalline anisotropy constants, θ and φ are elevation and azimuth angle of the magnetic moment, and Γ is the angle between the magnetic moment and magnetic field. Then, we can get the projected magnetization along a

magnetic field of arbitrary direction,

$$M(H) = A_0 \iint \mu_B g J \times \cos\Gamma \times \exp\left(-\frac{K_1 \sin^2\theta + K_2 \sin^4\theta - \mu_B g J \times H \cos\Gamma}{k_B T}\right) d\theta d\phi. \quad (4)$$

We used the measured magnetization (108.96 emu/g) in a field of 130 kOe along the c direction at 16 K to approximate the saturation magnetization $\mu_B g J$. Since the difference in magnetization between 15 and 17K is very small, the magnetization data at 16 K are approximately assumed to be the average magnetization data measured at 15 and 17 K, as shown in Fig. 6(a). By fitting the rotating magnetization data in a field of 50 kOe shown, as squares in Fig. 6(a), according to Eq. (4), we obtain values for K_1 and K_2 that are 1.49×10^8 and -6.7×10^7 erg/cm^3, respectively. The fitted result is displayed in Fig. 6(a) as a red line, which is in good agreement with the experimental data.

The magnetocrystalline anisotropy energy of $TmMnO_3$ in a field of 50 kOe for arbitratry direction can be written as

$$E_K = A_0 \iint (K_1 \sin^2\theta + K_2 \sin^4\theta) \times \exp\left(-\frac{K_1 \sin^2\theta + K_2 \sin^4\theta - \mu_B g J \times H \cos\Gamma}{k_B T}\right) d\theta d\phi. \quad (5)$$

As the magnetic field is rotated within the ac plane from the a to the c axis (i.e., from$[\theta = 90, \phi = 0]$ to $[\theta = \alpha, \phi = 0]$), the rotating field entropy change can be expressed as

$$-\Delta S^R(\alpha) = \int_{90}^{\alpha} -\frac{dE_K|_{H(\theta,0)}}{T} = -\frac{E_K|_{H(\alpha,0)} - E_K|_{H(90,0)}}{T}. \quad (6)$$

Figure 6(b) displays the result of Eq. (6) as a red line. The good consistence between the calculated result and experimental data obtained from the isothermal magnetization curves suggests that the giant anisotropy of the magnetocaloric effect in a $TmMnO_3$ single crystal with anisotropic paramagnetic response is attributed not only to the magnetocrystalline anisotropy, but also to thermal fluctuations.

IV. CONCLUSION

We investigated the anisotropy of entropy change $-\Delta S$ within the ac plane of a $TmMnO_3$ single crystal. The value of $-\Delta S$ along the c axis is much larger than that along the a axis in a temperature range of 2–50 K. By theoretical analysis of the rotating field entropy change $-\Delta S^R(\alpha)$ from the a to c axes at 16 K, we found that the contribution of the magnetocrystalline anisotropy is insufficient to account for the rotating field entropy change, and thermal fluctuations should be taken into account from the anisotropic paramagnetic response.

ACKNOWLEDGMENTS

This work was supported by the National Basic Research Program of China (973 program, Grant Nos. 2009CB929201, 2010CB934202, and 2011CB921801) and the National Natural Sciences Foundation of China (11174351, 50831006, 51021061, and 11034004).

*zhcheng@aphy.iphy.ac.cn

[1] V. D. Buchelnikov and V. V. Sokolovskiy, Phys. Metals Metallogr. **112**, 633 (2011).
[2] K. A. Gschneidner, V. K. Pecharsky, and A. O. Tsokol, Rep. Prog. Phys. **68**, 1479 (2005).
[3] B. G. Shen, J. R. Sun, and F. X. Hu, Adv. Mater. **21**, 4545 (2009).
[4] M. H. Phan and S. C. Yu, J. Magn. Magn. Mater. **308**, 325 (2007).
[5] S. A. Nikitin, K. P. Skokov, Y. S. Koshkid'ko, Y. G. Pastushenkov, and T. I. Ivanova, Phys. Rev. Lett. **105**, 137205 (2010).
[6] M. D. Kuz'min and A. M. Tishin, J. Phys. D: Appl. Phys. **24**, 2039 (1991).
[7] M. LoBue, V. Loyau, F. Mazaleyrat, A. Pasko, V. Basso, M. Kuepferling, and C. P. Sasso, J. Appl. Phys. **111**, 07A905 (2012).
[8] V. Basso, C. P. Sasso, M. Küpferling, K. P. Skokov, and O. Gutfleisch, J. Appl. Phys. **109**, 083910 (2011).
[9] J.-L. Jin, X.-Q. Zhang, G.-K. Li, Z.-H. Cheng, L. Zheng, and Y. Lu, Phys. Rev. B **83**, 184431 (2011).
[10] C. Meneghini, M. Maret, V. Parasote, M. C. Cadeville, J. L. Hazemann, R. Cortes, and S. Colonna, Eur. Phys. J. B **7**, 347 (1999).
[11] P. Blonski and J. Hafner, J. Phys. Condes. Matter **23**, 136001 (2011).
[12] R. Skomski and D. J. Sellmyer, J. Rare Earth **27**, 675 (2009).
[13] L. J. Wang, S. M. Feng, J. L. Zhu, Q. Q. Liu, Y. C. Li, X. D. Li, J. Liu, and C. Q. Jin, High Press. Res. **30**, 258 (2010).
[14] T. Katsufuji, M. Masaki, A. Machida, M. Moritomo, K. Kato, E. Nishibori, M. Takata, M. Sakata, K. Ohoyama, K. Kitazawa, and H. Takagi, Phys. Rev. B **66**, 134434 (2002).
[15] T. Jolicoeur and J. Le Guillou, Phys. Rev. B **40**, 2727 (1989).
[16] K. Uusi-Eskoa, J. Malmb, N. Imamuraa, H. Yamauchia, and M. Karppinena, Mater. Chem. Phys. **112**, 1029 (2008).
[17] J. S. Zhou, J. B. Goodenough, J. M. Gallardo-Amores, E. Morán, M. A. Alario-Franco, and R. Caudillo, Phys. Rev. B **74**, 014422 (2006).
[18] F. Yen, C. dela Cruz, B. Lorenz, E. Galstyan, Y. Y. Sun, M. Gospodinov, and C. W. Chu, J. Mater. Res. **22**, 2163 (2007).
[19] H. A. Salama and G. A. Stewart, J. Phys. Condens. Matter **21**, 386001 (2009).

[20] K. Yoshii and H. Abe, J. Solid State Chem. **165**, 131 (2002).
[21] V. Skumryev, M. D. Kuz'min, M. Gospodinov, and J. Fontcuberta, Phys. Rev. B **79**, 212414 (2009).
[22] K. A. Gschneidner Jr., V. K. Pecharsky, A. O. Pecharsky, and C. B. Zimm, Mater. Sci. Forum **315–317**, 69 (1999).
[23] A. Munoz, J. A. Aloñso, M. J. Martínez-Lope, M. T. Casáis, J. L. Martínez, and M. T. Fernández-Díaz, Chem. Mater. **13**, 1497 (2001).
[24] X. Fabrèges, I. Mirebeau, P. Bonville, S. Petit, G. Lebras-Jasmin, A. Forget, G. André, and S. Pailhès, Phys. Rev. B **78**, 214422 (2008).